

SUBCONTRACT TITLE: THE FABRICATION AND PHYSICS OF HIGH-EFFICIENCY CADMIUM – TELLURIDE THIN-FILM SOLAR CELLS

SUBCONTRACT NO: NDJ-1-30630-02

QUARTERLY TECHNICAL STATUS REPORT FOR: Phase 1/Quarter 2

SUBMITTED TO: Ken Zweibel
National Renewable Energy Laboratory

PRINCIPAL INVESTIGATORS: A.D. Compaan (P.I.) and V. G. Karpov (co-P.I.)
University of Toledo,
Department of Physics and Astronomy,
2801 W Bancroft,
Toledo, OH 43606

This progress report covers the second quarter of Phase 1 for the period December 01, 2001, through February 28, 2002.

This report describes our activities and progress in understanding of the effects of nonuniformities in CdTe photovoltaics. This includes PL mapping, light soaking of artificially nonuniform devices, and theoretical modeling. In our study we used VTD devices by First Solar, LLC and magnetron sputtered devices made at UT.

Our effort in studying effects of nonuniformities also extended to the National CdTe Team Meeting in Florida (March 2002) where we coordinated projects in the “Micrononuniformity” topical sub-team. The sub-team presented results on PL-mapping, μ -EL, μ -PL, μ -LBIC, GIXRD, AFM, EBIC, and CL. The UT group made five presentations during the meeting; (presenters: Diana Shvydka, A. Gupta, V. Karpov, A. Compaan).

PL mapping

PL mapping is aimed at characterizing the degree of device lateral uniformity in fresh and degraded samples with and without metal contacts. Room temperature PL was excited by a 752 nm laser with the beam spot size of $\sim 80 \mu\text{m}$ and step size of $200 \mu\text{m}$ in line scanning. We used two laser intensities: ~ 2000 sun and ~ 200 sun. Both the changes in PL spectra and total PL intensity were measured.

It was observed (Fig. 1) that the PL peak shifts to higher energy under the contact and, generally, the PL intensity is higher from contact-free area (first observed in Ref. [1]). While the latter observation was typical, some unusual samples were also found where applying metal did not have noticeable effect on PL. Considerable ($\sim 80\%$) of correlation was found between the maps corresponding to two different excitation powers.

Light soaking typically increased the ratio of PL intensities between the contact and metal-free areas, leaving other features practically intact (Fig. 2b).

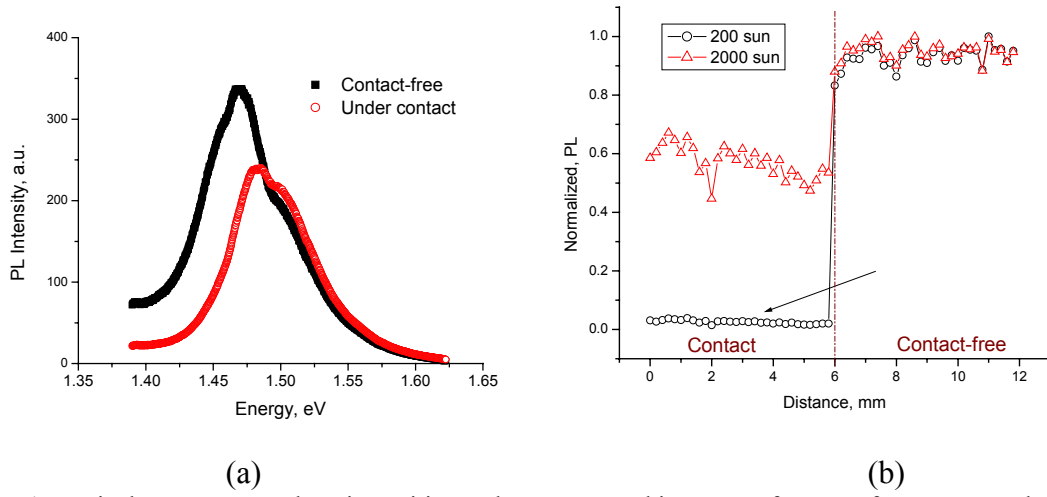


Fig. 1. Typical PL spectra and PL intensities under contact and in contact free area for VTD samples. PL intensities are shown for two different excitation powers in a fresh sample and are normalized to the maximum PL.

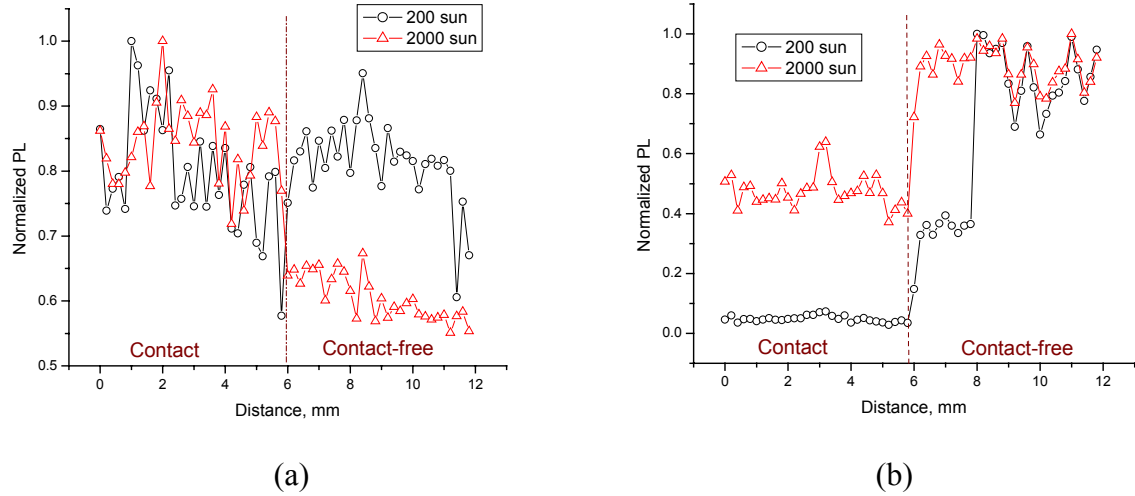


Fig. 2. PL mapping of “unusual” VTD fresh sample (a) and typical 28-day light soaked VTD sample (b) for two excitation powers.

Our interpretation of the contact/free area PL ratio is close to that in Ref. [1] and is illustrated in Fig. 3. The explanation assumes shunting pathways, whose influence extends greatly as the contact metal is applied, which turns the device into a short-circuit (SC) regime. Without the metal the device is largely under open circuit (OC) conditions. The latter makes the nonequilibrium electrons and holes accumulate, which suppresses the built-in electric field. Because the weaker field is less efficient in spatially separating the electrons and holes, they recombine more readily, thus increasing PL intensity.

An observation seemingly inconsistent with the above explanation was that the measured I/V curves did not exhibit characteristic shunting features. We therefore assume that shunting is due to weak micro-diodes [Ref. 2, 3] rather than to the standard ohmic shunts.

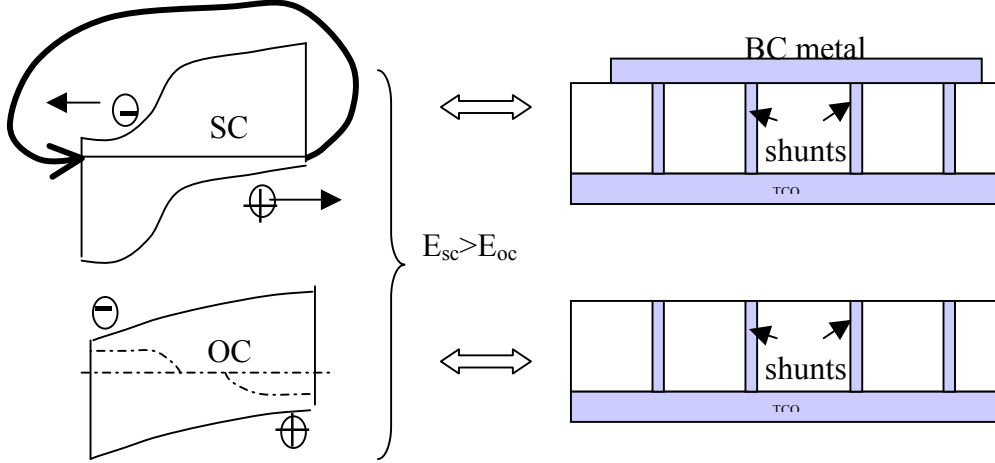


Fig. 3. Built-in electric field suppression by back-contact (BC) metal in a device with shunting pathways. The left side shows p-n junction band diagrams under short-circuit and open-circuit conditions. The right side illustrates short circuiting by a combination of shunting pathways and back contact metal.

For the magnetron-sputtered samples the shift in the spectrum was analogous to that of VTD samples (Fig. 1a), while PL maps turned out to be somewhat different as is illustrated in Fig. 4. In interpreting the difference we take into account that in magnetron sputtered samples the PL variations are due to a combination of two effects: (i) the presence of metal contact and (ii) local Cu doping under contact, as opposed to the VTD samples where both contact and contact-free areas are doped equally. Assuming Cu doping to increase PL efficiency, and applying metal to do the opposite, the PL under the contact in magnetron-sputtered samples will be affected by the above opposing factors. This may result in the contact-free area PL intensity to be less than under the contact. One indirect confirmation for the above interpretation follows from the ‘rabbit-ear’ feature at the contact edge in Fig. 4, which can be interpreted as the positive effect of Cu doping (diffused slightly beyond the contact) in the absence of the contact-metal negative effect.

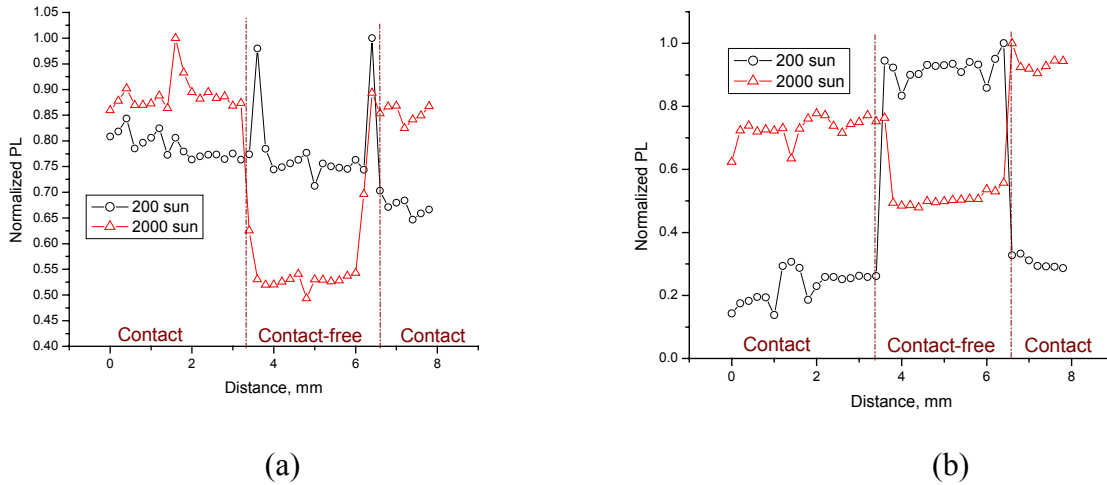


Fig. 4. PL mapping of magnetron-sputtered samples before (a) and after (b) 28-day light soak for two excitation powers.

Our conclusions on PL mapping can be summarized as follows: (i) PL mapping shows significant nonuniformities in both VTD and rf-sputtered, fresh and stressed devices. (ii) PL map topology generally depends on excitation power. (iii) There are substantial differences in PL intensities, spectra, and topologies between the contact and contact-free areas. (iv) The ratio of PL intensities from the contact and contact-free areas varies between samples. (v) There is no significant difference in PL spectra and degree of PL nonuniformity between fresh and stressed samples. (vi) Nonuniformities of different scale can be observed.

We plan to further extend the PL mapping technique capabilities by (1) studying it under applied bias, and (2) by developing a more quantitative interpretation.

Artificially nonuniform devices

We have carried out experiments in which solar cells were made artificially nonuniform before putting them under light soak. In a set of roundish CdTe/CdS dot cells, each cell was half shadowed along its diameter. After one-month light soak the screens were removed and the devices were scribed along their diameters, to make the former dark and light parts electrically disconnected. We have intentionally chosen devices with a broad range of deposition parameters: some of them degraded, while others improved under limited time exposure. As a control we light-soaked a number of fully open cells.

The data shown in Fig. 5 reveal that there was no preference of the light over the dark halves in the amount of degradation. This is consistent with the concept that it is not the light *per se*, but rather its generated forward electrical bias, which is responsible for the device degradation. The light-generated bias screening radius $L > 1$ cm, estimated from our original equations (Refs. [2, 3]) turns out to be long enough to let the bias spread over the entire cell.

In addition, Fig. 5b shows that, to the first approximation, the sum of the light and dark halves J_{sc} degradation is constant ($\sim 6-8\%$). The latter turns out to be larger by approximately a factor of two than that of our control fully open cells ($\sim 3-4\%$). This difference can be understood if J_{sc} degradation is significantly nonuniform and occurs in either half of the cell. The small current density degradation in the control cells is then explained by mistakenly relating the current degradation to the area that is overestimated by a factor of two (whole cell instead of half of a cell).

In general, the data in Fig. 5 reveal that there are degradation mechanisms of different length scales. In particular, V_{oc} degradation turns out to be more uniform than that of J_{sc} . This means that the bad diode contribution to the measured (average) V_{oc} is relatively immaterial, as opposed to the current, which is dominated primarily by the weakest diode in the system. This property of V_{oc} can be proven indeed by using the explicit (parabolic) coordinate dependence of the electric potential distribution caused by micro shunts.

The above experiments indicate that the cause for degradation is the light-generated forward bias and is consistent with the model of weak diodes being responsible for nonuniform degradation. Weak microdiodes (of low open-circuit voltage) were shown to affect macroscopically large regions where they strongly reduce the device performance and induce its nonuniform degradation in several different modes (Refs. [2,3]).

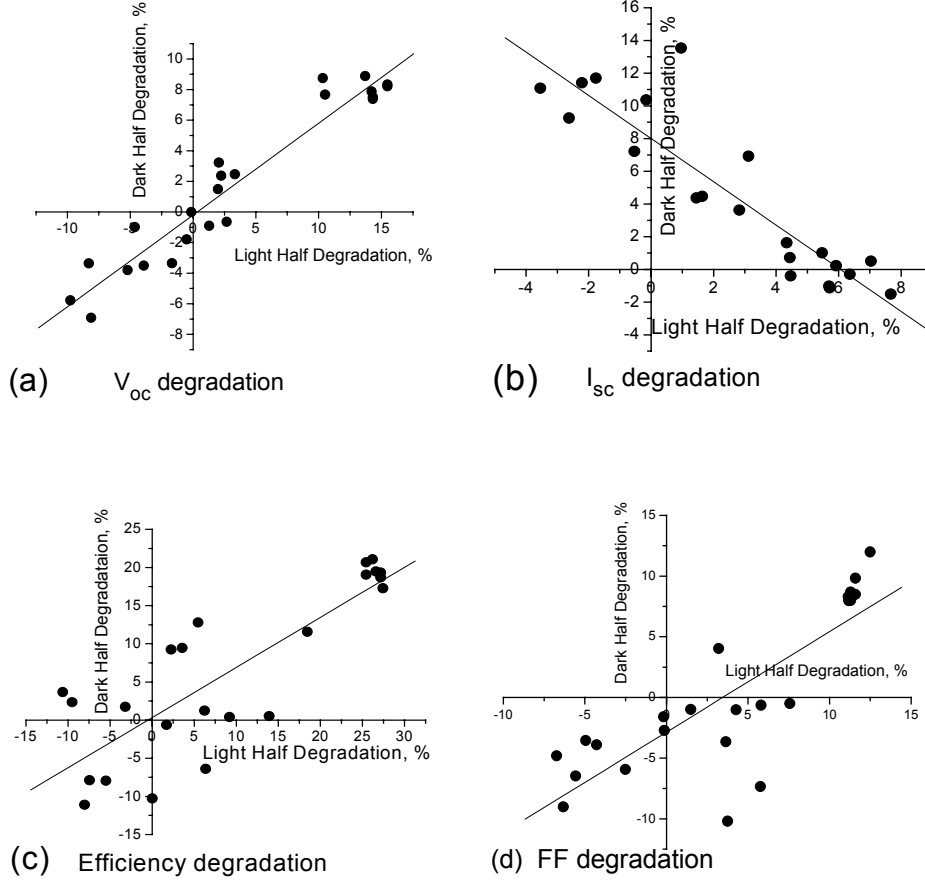


Fig. 5. Degradation of different parameters in a set of artificially nonuniform cells.

New experiments are now being designed to further verify the concept of nonuniform degradation. One such experiment is aimed at tracking nonuniformity in the cell corrosion, which process can start at weak micro-diodes and then spread over the entire system (Ref. 2). Also, additional degraded cell partitioning (in 4, 8, etc. parts) will show nonuniformity in degradation of different cell parameters.

Theoretical Modeling

We are putting a considerable effort into theoretical modeling of these micrononuniformities in thin-film photovoltaics. Our current activity concentrates on analytical and numerical modeling of lateral nonuniformity effects. The basic model is illustrated in Fig. 6. Each of the microdiode parameters (V_{oc} , R_{sc} , etc.) is considered random and is characterized by its corresponding average and dispersion. We have shown that fluctuations in V_{oc} are most crucial and are now studying their effects more in depth.

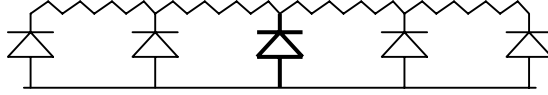


Fig. 6. Equivalent circuit of a laterally nonuniform device; microdiodes in parallel possess different parameters. The resistors represent TCO.

Our analytical modeling is aimed at deriving closed-form equations that describe the system integral parameters (macroscopically measured V_{oc} , etc.) in important limiting cases, such as the regime of weak fluctuations or the region of extremely strong, but unlikely fluctuations. We consider both 1D and 2D models. Our results (now being prepared for publication) show how the dispersion in the local V_{oc} causes loss in photocurrent, and which parameters of the device have more effect on the laterally nonuniform device efficiency.

For numerical simulations we have developed software that numerically evaluates the electric potential and current distributions in the circuit of Fig. 6 where the input is the microdiode parameter probabilistic distributions. This computer program is now being debugged and tested. We plan to make it available to the thin-film community by the end of this year by posting the program on our website. This will enable one to numerically model the effects of lateral nonuniformity depending on the material parameters characteristic for a particular class of thin-film photovoltaics.

References

- [1] D.H. Levi, L.M. Woods, D.S. Albin, T.A. Gessert, R.C. Reedy, and R.K. Ahrenkiel, presented at the 2nd World Conference on Photovoltaic Solar Energy Conversion, 1998, Vienna, Austria
- [2] V. G. Karpov, A. D. Compaan and Diana Shvydka, "Effects of Nonuniformities in Thin-Film Photovoltaics," *Appl. Phys. Lett.* **80**, p. 4256 (2002)
- [3] V. G. Karpov, A. D. Compaan and Diana Shvydka, "Micrononuniformity Effects in CdTe Photovoltaics," to be published in the 29th IEEE PVSC.